Optical Materials xxx (2013) xxx–xxx

Contents lists available at SciVerse ScienceDirect

Optical Materials

journal homepage: www.elsevier.com/locate/optmat

3D photografting with aromatic azides: A comparison between three-photon and two-photon case

Zhiquan Li [a,1], Aliasghar Ajami [b,1], Evaldas Stankevičius [c], Wolfgang Husinsky [b], Gediminas Račiukaitis [c], Jürgen Stampfl [d], Robert Liska [a], Aleksandr Ovsianikov [d,*]

[a] Institute of Applied Synthetic Chemistry, Vienna University of Technology, Getreidemarkt 9/163/MC, 1060 Vienna, Austria
[b] Institute of Applied Physics, Vienna University of Technology, Wiedner Hauptstrasse. 8, 1060 Vienna, Austria
[c] Center for Physical Sciences and Technology, Savanoriu Ave. 231, LT-02300 Vilnius, Lithuania
[d] Institute of Materials Science and Technology, Vienna University of Technology, Favoritenstrasse. 9-11, 1040 Vienna, Austria

ARTICLE INFO

Article history:
Available online xxxx

Keywords:
Femtosecond
Multi-photon
Patterning
Functionalization
Microfabrication
Grafting

ABSTRACT

Photografting is a method utilizing light activation for covalent incorporation of functional molecules to a polymer surface or polymer matrix. It has been widely applied as a simple and versatile method for tailoring physical–chemical properties of various surfaces. Grafting induced via multi-photon absorption provides additional advantages of spatial and temporal control of the process. Here, a novel fluoroaryl azide photografting compound (AFA) was synthesized and compared with the commercially available azide BAC-M. Using Z-scan technique, it was determined that AFA is a two-photon absorber at 798 nm, whereas BAC-M is a three-photon absorber at this wavelength. Both azides were employed for 3D photografting within a PEG-based matrix using femtosecond laser pulses. Both Z-scan measurements and 3D photografting tests indicated that, the intensity threshold for nonlinear absorption and photografting process is lower for AFA. As a result the processing window of AFA is much broader than that of BAC-M. But on the other hand, since BAC-M is characterized by the three-photon absorption (3PA) process, patterns with finer features can be produced using this molecule. The choice of the appropriate compound for 3D grafting will depend on the final application and the requirements associated with the resolution and post-modification protocol.

1. Introduction

Photografting is a method utilizing light activation for covalent incorporation of functional molecules to a polymer surface or polymer matrix. Arylazides have been widely used to tailor various surfaces (e.g. glass [1], carbon [2] and metals [3]) for specific applications ranging from electronic to biomedical engineering [1]. Among various strategies developed for the surface modification by arylazides, photografting is especially promising due to its versatility and simplicity [4]. The photografting patterns could be customer-made by using masks or stamps or by standard photolithographic procedures [5]. Moreover, spatial and temporal control of the photografting process can be realized simply by tuning the exposure dose [6]. Due to technical limitations, most studies on photografting are concerned with two dimensional patterning of surfaces. However, capability to produce volumetric patterns decorated with biomolecules is very attractive for tissue engineering, as it provides the possibility to tailor the *in vitro* model much closer to the real 3D appearance of the natural extracellular matrix [7,8]. Multi-photon grafting (MPG) stands out due to its potential to immobilize functional molecules within a 3D volume in a straightforward fashion [8]. In addition, since multi-photon-induced reactions are confined within the small focal volume, very precise functionalization can be achieved with high resolution [9,10].

Our recent work has proved the concept by employing commercial arylazide BAC-M (Fig. 1) for selective functionalization of 3D PEG matrix under three-photon irradiation [8]. The obtained results encouraged us to explore more aromatic azides for 3D photografting via multi-photon excitation.

Molecule design of arylazide is critical for the efficiency of MPG process. Efficient grafting reagent requires large multi-photon absorption (MPA) cross-section combined with high photografting efficiency. Chromophores with large MPA cross-section are characterized by a planar π conjugated system containing electron donor (D) and acceptor (A) groups [11]. However, the synthesis of arylazide with complex structures possessing large MPA has remained a serious challenge until now due to the high sensitivity and explosive nature of azides [12]. Here, we report a novel fluoroaryl azide AFA (Fig. 1) straightforwardly synthesized under mild condition with satisfying yield. A C=N bond was selected as π bridge due

* Corresponding author. Tel.: +43 1 58801 30830.
E-mail address: Aleksandr.Ovsianikov@tuwien.ac.at (A. Ovsianikov).
[1] These authors contributed equally to this work.

0925-3467/$ - see front matter © 2013 Elsevier B.V. All rights reserved.
http://dx.doi.org/10.1016/j.optmat.2013.04.007

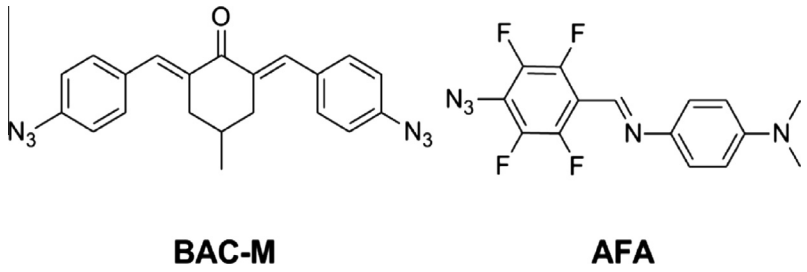

Fig. 1. Structures of the investigated aromatic azides.

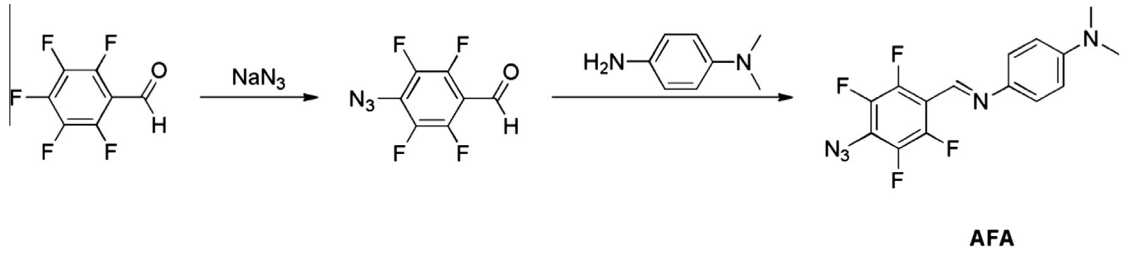

Fig. 2. Reaction scheme for the synthesis of the new arylazide.

to its nearly identical contribution to MPA cross-section compared to the C=C bond analogues [13] but much simpler synthesis. The formation of C=C bonds is mostly realized by classical Wittig or Horner–Wadsworth–Emmons reaction under strong alkaline conditions. The generated mixture of cis- and trans- isomers makes the purification process more difficult. However, C=N bonds could be formed under mild condition with satisfying yield and the impurity could be simply washed away with corresponding solvents. In addition, a C=N bond is potentially hydrolysable under acidic conditions. The aldehyde group generated after hydrolysis provides possibility for post-functionalization via oxime click chemistry [14]. N,N-dimethylaniline and fluorinated aromatic azide were selected as D and A groups, respectively. Beside the strong electron drawing ability of fluoroaryl azides such series compounds offer high grafting efficiency because of the selective formation of singlet nitrene intermediates which exclude potential deactivations derived from intra-molecular rearrangement [15].

The open aperture Z-scan measurements [16] were carried out to evaluate the nonlinear absorption properties of the novel azide AFA. In order to study the grafting efficiency and determine the processing window, MPG tests were performed using different average laser powers and scanning speeds. The obtained results were compared with the three-photon active aromatic azide BAC-M [17].

2. Experimental

2.1. Materials

All reagents for synthesis were purchased from Sigma–Aldrich and were used without further purification. The solvents were dried and purified by standard laboratory methods.

2.2. Synthesis

2.2.1. 4-Azido-2,3,5,6-tetrafluorobenzaldehyde

About the paragraph 0.30 g (4.6 m mol) of NaN_3 and 0.88 g (4.3 m mol) of pentafluorobenzaldehyde were dissolved in a mixture of acetone (8 mL) and water (3 mL). The solution was refluxed for 8 h, then cooled to room temperature, diluted with water (10 mL), and extracted by ether (3 × 10 mL). The extract was dried over $MgSO_4$ and evaporated. Purification by sublimation (25 °C/0.1 mm) yielded 0.78 g of product (80%) as white crystalline. Mp: 43–44 °C (Lit [15]: 44–45 °C). ^{1}H NMR (200 MHz, $CDCl_3$): δ (ppm) = 10.24 (s, 1H, CHO). IR (cm^{-1}): 2118, 1707, 1644, 1480, 1399, 1234, 1092, 982.

2.2.2. N^1-(4-azido-2,3,5,6-tetrafluorobenzylidene)-N^4,N^4-dimethylbenzene-1,4-diamine (AFA)

About the paragraph 0.21 g (1 m mol) of 4-azido-2,3,5,6-tetrafluorobenzaldehyde and 0.20 g (1.5 m mol) of N,N-dimethylbenzene-1,4-diamine were dissolved in dry toluene. The solution was stirred overnight under room temperature and then the solvent was evaporated under vacuum. The dark mixture was washed with dry acetone to yield 0.16 g (50%) of product as orange powder. Mp: 141–143 °C (decomposition). ^{1}H NMR (200 MHz, $CDCl_3$): δ (ppm) = 8.61 (s, 1 H, CH=N), 7.31 (d, J = 9.0 Hz, 2 H, Ar–H), 6.75 (d, J = 9.0 Hz, 2 H, Ar–H), 3.02 (s, 6 H, CH_3). ^{13}C NMR (50 MHz, $CDCl_3$): δ (ppm) = 150.4, 146.9–141.0 (m, F–C), 139.8, 122.7, 112.4, 112.0 40.5. IR (cm^{-1}): 2112, 1616, 1591, 1562, 1512, 1471, 1342, 1222, 1008, 823. Anal. Calcd for $C_{15}H_{11}F_4N_5$: C, 53.42; H, 3.29; N, 20.76; Found: C, 53.18; H, 3.48; N, 20.53.

2.3. Characterization

^{1}H NMR (200 MHz) and ^{13}C NMR (50 MHz) spectra were measured with a BRUKER ACE 200 FT–NMR-spectrometer. The chemical shift (s = singlet, bs = broad singlet, d = doublet, t = triplet, m = multiplet) is stated in ppm using the nondeuterated solvent as internal standard. Solvents with a grade of deuteration of at least 99.5% were used. Melting points were measured on a Zeiss axioscope microscope with a Leitz heating block and remained uncorrected. Elemental microanalysis was carried out with an EA 1108 CHNS–O analyzer from Carlo Erba at the microanalytical laboratory of the Institute for Physical Chemistry at the University of Vienna.

A Ti: sapphire laser system (25 fs pulse duration, 1 kHz repetition rate at 798 nm) was used for the open aperture Z-scan analysis. A detailed description of the setup and laser pulse and beam char-

acterization can be found elsewhere [18]. Both azide compounds were prepared as 1.0×10^{-2} M solutions in spectroscopic grade dimethylformamide (DMF). The sample solutions were measured in a 0.2 mm thick flow cell in a non-recycling volumetric flow of 4 mL/h. The measurements were carried out at different pulse energies in the range of 20–220 nJ corresponding to intensities ranging from 0.11 TW/cm^2 to 1.2 TW/cm^2. The used intensities were limited in this range since, at higher intensities the solvent contributes to the effective nonlinear absorption and at lower intensities no nonlinear absorption was observed. Another limit also arises from fitting process used in the Z-scan method. The laser light intensity should be kept below an amount so that the normalized transmittance stays above 76%.

2.4. Multi-photon grafting

The samples were prepared from poly(ethylene glycol) diacrylate (PEGda, average M_n 700, Sigma Aldrich) and DMF mixture (ratio 50:50) with an addition of 1 wt.% of the photoinitiator Irgacure819 (Ciba Specialty Chemicals Inc.). The resulting formulation was photopolymerized with UV light for 5 min (Intelliray 600) in silicone molds (diameter 6 mm; thickness 1 mm). The photopolymerized material pellets were soaked in DMF solution for at least 1 week, with the solvent being exchanged on a regular basis, in order to remove residual monomer and photoinitiator. For laser photografting, the samples were immersed into the 14 m mol/L solution of BAC-M or AFA in DMF. A Ti:sapphire femtosecond laser (High Q, Femtotrain), emitting pulses with duration of 80 fs at a 73 MHz repetition rate around 793 nm was used for laser grafting. The laser beam was focused with a 20 × microscope objective (Zeiss, NA = 0.8) into the sample. An acousto-optical modulator was used for fast switching of the laser beam and for adjusting its intensity. The laser power was measured before the objective. The patterns were obtained by scanning the focused laser beam within the sample by the galvo-scanner (HurryScan, ScanLab). The grafted patterns were produced by a set of adjacent line scans: Fig. 6a and c at a distance of 1.5 μm; and, Fig. 6b and d at a distance of 3 μm and 4.5 μm, respectively. In the vertical direction a step of 5 μm (total 7 slices) was used. After the grafting procedure, the samples were placed in DMF in order to remove the residual BAC-M or AFA. Rapid decoloration of the pellet indicated the successful removal of possible residuals from the sample. The fluorescence of the patterned samples was analyzed by laser scanning microscopy (LSM700 ZEN software, Carl-Zeiss) at the excitation wavelength of 555 nm.

3. Results and discussion

3.1. Synthesis and characterization

For the synthesis of the functional AFA, the preparation of the precursor azidotetrafluorobenzaldehyde has been well developed [16]. With strong electron-withdrawing property, pentafluorobenzaldehyde was reacted with the nucleophilic reagent sodium azide under reflux acetone/water mixture to give the desired aledhyde with high yield (80%). It is reported that no ortho-isomer was detected with such synthesis procedure [15] and our characteristic data are in well agreement with the previous reports [19]. The azide precursor was then reacted with N,N-dimethyl-benzene-1,4-diamine at room temperature, forming AFA with satisfying yield (50%) (see Fig. 2). Pure product could be obtained by simply washing with cold acetone. The characteristic peak of azide group at 2112 cm^{-1} in infrared spectra indicates the product with the desired functional group.

3.2. Z-scan measurements

To investigate the nonlinear absorption properties of the utilized azides, an open aperture Z-scan analysis was performed at 798 nm. A 0.2 mm thick cell in nonrecycling flow geometry was used for the measurements. A 4 ml/h flow was determined as an optimal flow rate to refresh the sample in the laser intersection region in order to avoid any negative effect derived from photodegradation during the tests and to prevent wasting too much compound as well. The laser beam of 15 mm diameter was focused by a 300 mm focal length lens leading to a 0.86 mm Rayleigh length considering a beam quality factor of 2. Thus, the thin sample criterion required for applying the Z-scan technique is fulfilled since the Rayleigh length is four times larger than the thickness of the sample. The solvent (DMF) was examined prior to measuring the samples to determine the intensity at which it starts to show nonlinear absorption. It was verified that no nonlinear absorption occurs in this solvent for pulse energies lower than 230 nJ hence, the Z-scan experiments with both azide compound were carried out for pulse energies below 230 nJ. In order to determine the order of MPA and also to verify the occurrence of excited state absorption, a series of Z-scans with different pulse energies were performed for each compound (Fig. 3). Eqs. (1) and (2) (see Appendix A) are the appropriate theoretical curves for fitting to the Z-scan data to extract the 2PA and 3PA cross-sections respectively.

In the Z-scan method, the absorbance caused by the third-order nonlinearities such as 2PA is proportional to the input intensity while the one resulted from the fifth-order nonlinearities such as 3PA is quadratic to the input intensity [20]. As seen from Z-scans of AFA shown in Fig. 3b the maximum transmittance (at focus) behaves linearly with pulse energy which is an indication of 2PA process. The maximum transmittance in Z-scans of BAC-M increases quadratically with pulse energy signifying the predominance of 3PA process in this compound. From Eqs. (1) and (2) (see Appendix A) it is derived that the slope of $\mathrm{Log}(1-T)$ versus $\mathrm{Log}(E)$ is 1 for TPA process and 2 for 3PA process. This is illustrated in Fig. 4b confirming the predominance of 2PA process in AFA and 3PA in BAC-M. From fitting Eq. (1) to Z-scans of AFA (Fig. 3b) the 2PA cross-section was extracted 1.78×10^{-48} cm^4 s (178 GM) for this compound that is relatively high compared to results found in the literature [21] since the molecule contains "push–pull" structure employing fluoroaryl azide as acceptor, dimethylamino group as donor and double bonds as conjugation bridge. The 3PA cross-section for BAC-M was extracted 1.19×10^{-78} cm^6 s^2 from fitting to the Z-scans data (Fig. 3a) using Eq. (2).

Fig. 4a shows two Z-scans of AFA and BAC-M with the same transmittance. It indicates that the intensity required to cause a certain absorbance via a 2PA process is much lower than that of a 3PA process. It also illustrates the main advantage of a three-photon absorber over a two-photon absorber. The transmittance change versus intensity is faster in case of 3PA comparing to 2PA leading to achieve higher spatial resolution in MPG using three-photon grafting molecules. These two major differences between a two-photon absorber and a three-photon absorber (i.e. lower intensity threshold for starting 2PA but higher structural resolution using a three-photon absorber in MPG) were practically illustrated by performing photografting patterning tests using AFA and BAC-M (see next section). Figs. 7 and 8 of Appendix A also show how two-photon and three-photon absorbance is distributed spatially along both lateral and axial directions that leads to smaller width for grafted lines produced via 3PA.

3.3. Comparison of multi-photon grafting with BAC-M and AFA

Although two-photon induced reactions and one photon induced reactions differ on the initiation stage, the subsequent

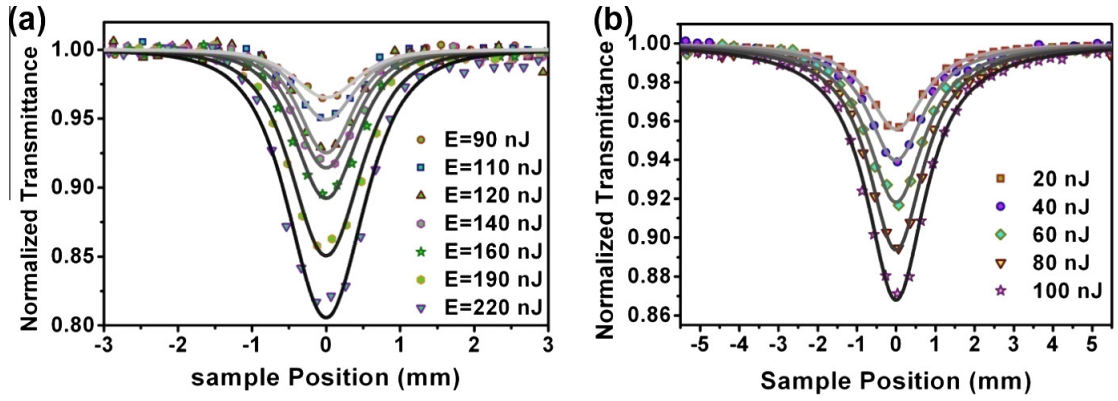

Fig. 3. (a) Experimental Z-scan data (dots) and fitting curves (full lines) for BAC-M (a) and AFA (b) at different pulse energies.

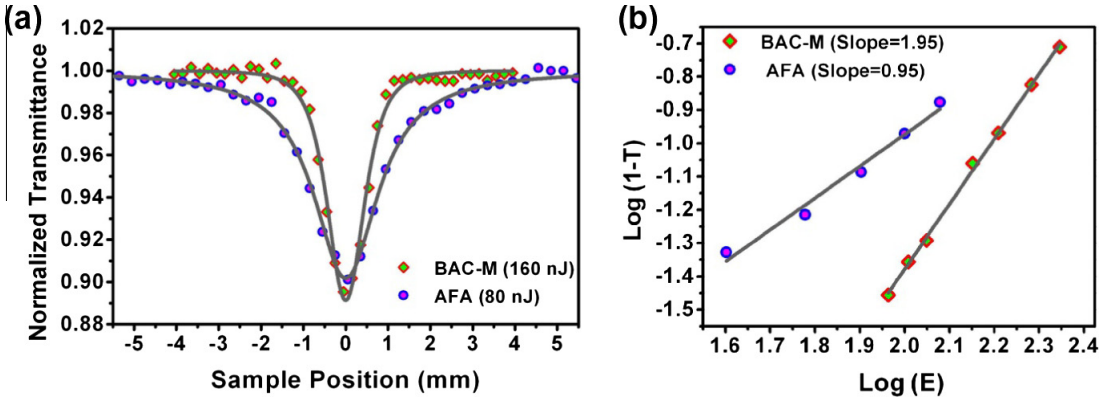

Fig. 4. (a) Z-scans of BAC-M and AFA with the same transmittance. (b) Log$(1-T)$ versus Log(E) for both compounds indicating that BAC-M is a three-photon absorber but AFA is a two-photon absorber.

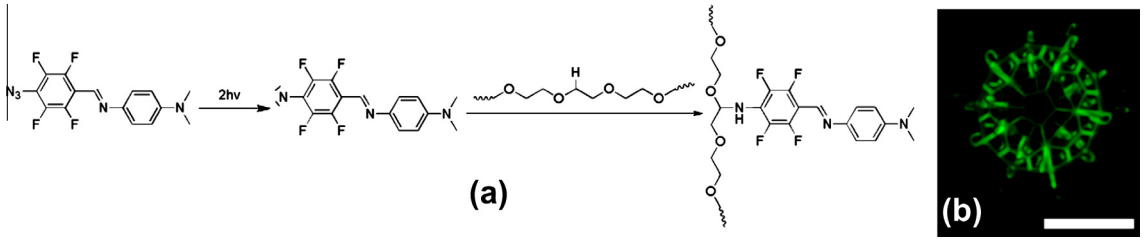

Fig. 5. Grafting process: (a) 2PA-induced photolysis of AFA, followed by an insertion reaction within the PEG-based matrix; (b) fluorescent image of a photografted lockyball [21]. Scale bar 200 μm.

grafting process is expected to be the same. The focused laser beam interacts with AFA via 2PA (Fig. 5). Photolysis of the azide causes the dissociation of the N–N bond from the excited singlet state followed by the generation of nitrogen and nitrene species. The highly reactive nitrene intermediate could undergo various reactions and Fig. 5 depicts the desired one: direct immobilization on the PEG-network by insertion into a C—H bond. This single step process is very universal because it is applicable to a wide variety of matrices containing C—H or N—H bonds. Since the PEG is transparent in near infrared spectral range, the pulsed laser beam is able to penetrate deeply into the matrix and induce the photografting reactions within 3D volume of the sample. Moreover, since the multi-photon interaction is confined within the small focal volume, more accurate immobilization of azide molecules (AFA or BAC-M) on the PEG matrix could be obtained. During grafting, the chromophore is covalently linked to the matrix. The grafting products still contain "push–pull" features, which exhibit certain fluorescence. Therefore, grafted patterns can be directly visualized via laser-scanning microscopy (LSM). Fig. 5b shows an LSM image of a 3D lockyball pattern [22] produced with AFA (0.5%) at the average power of 330 mW and scanning speed of 500 mm/s.

Both AFA and BAC-M contain active arylazide groups for MPG. Since the activation of AFA is under two-photon excitation, while BAC-M has proven to be three-photon active, it is of interest to compare the photografting behavior of these aromatic azides under different order of excitation. Fig. 6a and c shows the processing windows of both arylazides using different average laser powers and scanning speeds. The probability of 3PA is lower than that of 2PA; as a consequence higher laser intensity is required for the activation of BAC-M compared to AFA. This difference in the threshold is confirmed by the fact that the MPG processing window of AFA is much broader than that of BAC-M, allowing creation

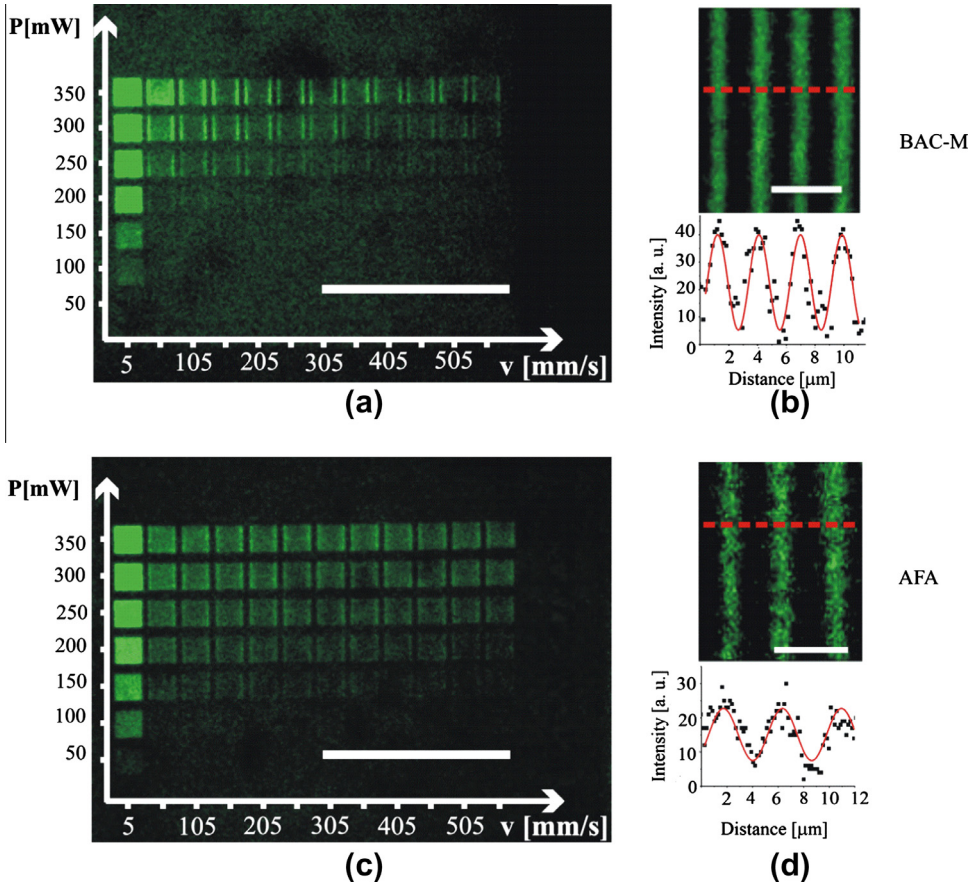

Fig. 6. An array of multi-photon grafted patterns produced at the different scanning speed and average laser power: (a) BAC-M and (c) AFA. The scale bar is 500 μm. Comparison of achievable resolution; the distance between lines is: (b) 3 μm for BAC-M and (d) 4.5 μm for AFA. The scale bar is 5 μm.

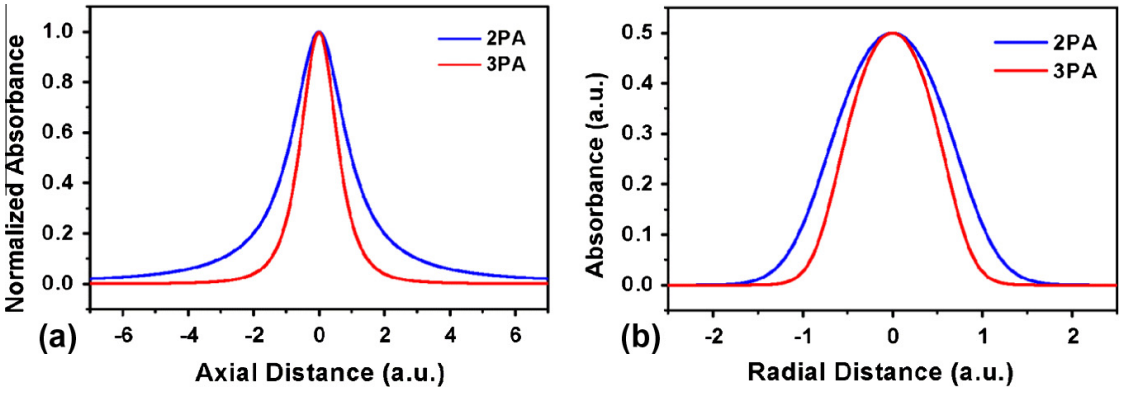

Fig. 7. (a) The axial distribution and (b) the radial distribution of the absorbance for both 2PA and 3PA process.

of photografted patterns with lower intensity and with higher writing speed using AFA. However, the observed fluorescence intensities of grafted patterns of BAC-M under high laser intensities and low scanning speed are greater than those of AFA with the identical parameters. This difference can be explained by the photografting products of BAC-M, which contain the ketocyanine chromophore with strong fluorescence [23]. Notably, the levels of immobilization can be spatially controlled by simply altering the irradiation exposure time or laser intensity during the photopatterning process, as demonstrated in Fig. 6. Such controlled 3D spatial gradients cannot be generated by conventional photolithographic methods. The ability to produce biochemical and biomechanical gradients in 3D is important to numerous bio-technology applications [24].

The achievable resolution for BAC-M and AFA patterns produced at fixed grafting parameters (the average laser power of 350 mW and laser scanning speed of 5 mm/s) and molar concentration of azides molecules (14 m mol/L) was also compared (Fig. 6). It was evaluated that the width of single lines produced by using the above mentioned laser power and scanning parameters is around 2.5 μm for BAC-M and around 4.1 μm for AFA. The resolvability of lines is confirmed by the according fluorescence intensity distribution. At a smaller distance the separate lines could not be distinguished. BAC-M shows a better spatial

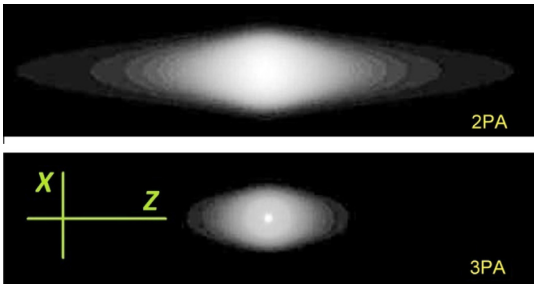

Fig. 8. Simulated 2D distribution of the absorbance corresponding to the cross-section of the produced lines via MPG using two-photon absorber grafting molecules (above) and three-photon absorber grafting molecules (below).

resolution than AFA. Since the immobilization of BAC-M molecule proceeds via 3PA process and of AFA via 2PA process, the initial activation volume is expected to be smaller for BAC-M.

4. Conclusion

A novel photografting compound AFA, which contains fluoroaryl azide as acceptor, dimethylamino group as donor and N=C double bonds as π conjugation bridge, was synthesized and evaluated. Using Z-scan method the order of nonlinear absorption of AFA was determined 2PA and an according absorption cross-section of 178 GM at 798 nm. Comparison between the AFA and BAC-M (a commercial 3PA active azide) demonstrated that the intensity required to induce multi-photon absorption in AFA is a few times lower than for BAC-M. As a consequence the AFA exhibits larger processing window and supports higher writing speed in photografting process. However, due to the 3PA interaction nature, the volume in which BAC-M molecules are excited can be more confined. This is the advantage of BAC-M over AFA since it leads to higher patterning resolution in MPG. The presented method is not confined to PEG-based matrix, but extensively applicable to various transparent matrices containing C—H or N—H bonds. Straightforward synthesis along with high scanning speed of over 550 mm/s indicate the great potential of AFA for possible applications in studies of cell-surface interactions, drug screening, sensing applications and microarray-based proteome analysis.

Acknowledgments

The authors acknowledge the financial support by the China Scholarship Council (CSC, No. 2009688004). E. Stankevičius would like to thank the Research Council of Lithuania for given financial support by Agreement No. SDS-2012-032. Dr. A. Ovsianikov would like to acknowledge financial support by the European Research Council under the EU FP7 (ERC Starting Grant no. 307701).

Appendix A

The normalized transmittance in the open aperture Z-scan technique is given by the following Eqs. (1) and (2) for 2PA and 3PA process respectively.

$$T(z) = \sum_{n=0}^{\infty} \frac{(-q_0)^n}{(n+1)^{3/2}(1+x^2)^n} \tag{1}$$

$$T(z) = \sum_{m=0}^{\infty} \frac{(-1)^m p_0^{2m}}{(2m+1)1/2(x^2+1)^{2m}} \tag{2}$$

where $q_0 = (\sigma_2 N_A \rho \times 10^{-3}/\hbar\omega) L i_0$, $p_0 = \sqrt{2(\sigma_3 N_A \rho \times 10^{-3}/(\hbar\omega)^2) L I_0}$, $x = z/z_0$, z is the sample position, z_0 is the Rayleigh length, N_A is the Avogadro number, ρ is the concentration of compound in mole per liter, ω is the angular frequency of the laser radiation, $\hbar$ is the reduced Plank constant, L is the thickness of the sample, I_0 is the maximum intensity at the focus, σ_2 is the 2PA cross-section and σ_3 is the 3PA cross-section.

The transmitted intensity through a nonlinear medium is given by the following Eqs. (3) and (4) for 2PA and 3PA process respectively.

$$I_e(z,r,t) = \frac{I(z,r,t)}{1+\alpha_2 L I(z,r,t)} \tag{3}$$

$$I_e(z,r,t) = \frac{I(z,r,t)}{\sqrt{1+2\alpha_3 L I^2}} \tag{4}$$

From Eqs. (1)–(4) the absorbance can be derived as a function of distance measured with respect to the focal point in both lateral and axial direction for both 2PA and 3PA process. This is shown in Figs. 7 and 8. Fig. 8 shows a simulated 2D absorbance distribution for both 2PA and 3PA. The scanning direction is perpendicular to the figure plane hence these absorbance distributions show how the cross-section of the grafted lines via 3PA differs from that of 2PA.

References

[1] D. Samanta, A. Sarkar, Chemical Society Reviews 40 (2011) 2567–2592.
[2] S.J. Pastine, D. Okawa, B. Kessler, M. Rolandi, M. Llorente, A. Zettl, J.M.J. Fréchet, Journal of the American Chemical Society 130 (2008) 4238–4239.
[3] E.W. Wollman, D. Kang, C.D. Frisbie, I.M. Lorkovic, M.S. Wrighton, Journal of the American Chemical Society 116 (1994) 4395–4404.
[4] M.A. Holden, P.S. Cremer, Journal of the American Chemical Society 125 (2003) 8074–8075.
[5] M. Busson, A. Berisha, C. Combellas, F. Kanoufi, J. Pinson, Chemical Communications 47 (2011) 12631–12633.
[6] C.B. Herbert, T.L. McLernon, C.L. Hypolite, D.N. Adams, L. Pikus, C.C. Huang, G.B. Fields, P.C. Letourneau, M.D. Distefano, W.S. Hu, Chemistry and Biology 4 (1997) 731–737.
[7] A.M. Kloxin, M.W. Tibbitt, K.S. Anseth, Natural Protocols 5 (2010) 1867–1887.
[8] A. Ovsianikov, Z. Li, J. Torgersen, J. Stampfl, R. Liska, Advanced Functional Materials 22 (2012) 3429–3433.
[9] A. Ovsianikov, V. Mironov, J. Stampf, R. Liska, Expert Review of Medical Devices 9 (2012) 613–633.
[10] R.G. Wylie, S. Ahsan, Y. Aizawa, K.L. Maxwell, C.M. Morshead, M.S. Shoichet, Natural Materials 10 (2011) 799–806.
[11] Z. Li, M. Siklos, N. Pucher, K. Cicha, A. Ajami, W. Husinsky, A. Rosspeintner, E. Vauthey, G. Gescheidt, J. Stampfl, R. Liska, Journal of Polymer Science, Part A: Polymer Chemistry 49 (2011) 3688–3699.
[12] S. Bräse, C. Gil, K. Knepper, V. Zimmermann, Angewandte Chemie International Edition 44 (2005) 5188–5240.
[13] L. Antonov, K. Kamada, K. Ohta, F.S. Kamounah, Physical Chemistry Chemical Physics 5 (2003) 1193–1197.
[14] G.N. Grover, J. Lam, T.H. Nguyen, T. Segura, H.D. Maynard, Biomacromolecules 13 (2012) 3013–3017.
[15] J.F.W. Keana, S.X. Cai, The Journal of Organic Chemistry 55 (1990) 3640–3647.
[16] M. Sheik-Bahae, A.A. Said, T.-H. Wei, D.J. Hagan, E.W. Van Stryland, IEEE Journal of Quantum Electronics 26 (1990) 760–769.
[17] A. Ovsianikov, Z. Li, A. Ajami, J. Torgersen, W. Husinsky, J. Stampfl, R. Liska, Applied Physics A: Materials Science and Processing 108 (2012) 29–34.
[18] A. Ajami, W. Husinsky, R. Liska, N. Pucher, Journal of the Optical Society of America B: Optical Physics 27 (2010) 2290–2297.
[19] S.J. Lord, H.-I.D. Lee, R. Samuel, R. Weber, N. Liu, N.R. Conley, M.A. Thompson, R.J. Twieg, W.E. Moerner, The Journal of Physical Chemistry B 114 (2009) 14157–14167.
[20] C. Lu, Y. Cui, B. Gu, F. Wang, Journal of Nonlinear Optical Physics and Materials 19 (2010) 327–338.
[21] K.J. Schafer, J.M. Hales, M. Balu, K.D. Belfield, E.W. Van Stryland, D.J. Hagan, Journal of Photochemistry and Photobiology A: Chemistry 162 (2004) 497–502.
[22] R.A. Rezende, F.D.A.S. Pereira, V. Kasyanov, A. Ovsianikov, J. Torgensen, P. Gruber, J. Stampfl, K. Brakke, J.A. Nogueira, V. Mironov, J.V.L. da Silva, Virtual and Physical Prototyping 7 (2012) 287–301.
[23] J.M. Eisenhart, A.B. Ellis, Journal of Organic Chemistry 50 (1985) 4108–4113.
[24] M.S. Hahn, J.S. Miller, J.L. West, Advanced Materials 18 (2006) 2679–2684.